

ARTICLE OPEN



Robust entanglement distribution via telecom fibre assisted by an asynchronous counter-propagating laser light

Koichiro Miyanishi^{1✉}, Yoshiaki Tsujimoto^{1,2}, Rikizo Ikuta^{1,3}, Shigehito Miki^{4,5}, Masahiro Yabuno⁴, Taro Yamashita^{6,7}, Hiroataka Terai⁴, Takashi Yamamoto^{1,3}, Masato Koashi⁸ and Nobuyuki Imoto^{3,9}

Distributing entangled photon pairs over noisy channels is an important task for various quantum information protocols. Encoding an entangled state in a decoherence-free subspace (DFS) formed by multiple photons is a promising way to circumvent the phase fluctuations and polarisation rotations in optical fibres. Recently, it has been shown that the use of a counter-propagating coherent light as an ancillary photon enables us to faithfully distribute entangled photon with success probability proportional to the transmittance of the optical fibres. Several proof-of-principle experiments have been demonstrated, in which entangled photon pairs from a sender side and the ancillary photon from a receiver side originate from the same laser source. In addition, bulk optics have been used to mimic the noises in optical fibres. Here, we demonstrate a DFS-based entanglement distribution over 1 km optical fibre using DFS formed by using fully independent light sources at the telecom band, and obtain a high-fidelity entangled state. This shows that the DFS-based scheme protects the entanglement against collective noise in 1 km optical fibre. In the experiment, we utilise an interference between asynchronous photons from continuous wave pumped spontaneous parametric down conversion (SPDC) and mode-locked coherent light pulse. After performing spectral and temporal filtering, the SPDC photons and light pulse are spectrally indistinguishable. This property allows us to observe high-visibility interference without performing active synchronisation between fully independent sources.

npj Quantum Information (2020)6:44; <https://doi.org/10.1038/s41534-020-0273-5>

INTRODUCTION

Sharing entanglement between two distant parties is an important prerequisite to realise quantum internet^{1,2}, including quantum key distribution^{3,4}, quantum repeaters⁵ and quantum computation between distant parties^{6,7}. For this purpose, entanglement is embedded in a suitable degree of freedom of single photons, e.g. polarisation, time and so on. When we look at a fibre-based entanglement distribution, temporal degree of freedom (time-bin qubit)⁸ has often been employed due to the robustness against phase fluctuations and/or polarisation rotations in the optical fibre^{9–11}. However, subwavelength-level-stabilised interferometers are necessary in distant parties, and stabilisation of these interferometers is not always practical. Another way to share entangled photons is the use of a polarisation degree of freedom (polarisation qubit), which is easy to be generated, manipulated and measured. The drawback is the susceptibility to the noises in the optical fibre. Although several experiments have demonstrated the passive polarisation entanglement distribution through an optical fibre, the situation was limited to the cases using stable fibres such as fibre spools¹² and submarine cables¹³. Given more practical situations where the environment surrounding the optical fibre is not stable, the use of a decoherence-free subspace (DFS) formed by n photons is a useful way¹⁴. Notably, the DFS scheme is more stable than the time-bin scheme, because it uses two-photon interference and does not need

subwavelength-level-stabilisation of the interferometer. So far, many types of DFS-based photon distributions have been experimentally demonstrated^{15–24}. A drawback of such DFS protocols is that the efficiency is proportional to n th power of channel transmittance and thus the communication distance is severely limited. In ref. ²⁵, the efficiency of DFS against phase disturbance has been improved to be proportional to the channel transmittance with the use of a counter-propagating laser light for the ancillary photon from the receiver to the sender. Recently, the method was applied to general collective noise by introducing two independent transmission channels^{26,27}. In these improved DFS schemes, quantum interference between the idler photon and the coherent light pulse is used. In practice, the signal photon and the light pulse are expected to be prepared independently by the sender and by the receiver. However, in the demonstrations^{25,27}, the signal photon and the light pulse were prepared from the same laser source as is the case of the original DFS protocols in which both the signal and the ancillary photons are prepared by the sender. In addition, these experiments are performed in free space with bulk optics simulating the noises and losses of the optical fibres.

In this paper, we report DFS-protected entanglement distribution through optical fibres by preparing the signal and the ancillary photons from fully independent telecom light sources. We use entangled photon pairs prepared by continuous

¹Graduate School of Engineering Science, Osaka University, Toyonaka, Osaka 560-8531, Japan. ²Advanced ICT Research Institute, National Institute of Information and Communications Technology (NICT), Koganei, Tokyo 184-8795, Japan. ³Center for Quantum Information and Quantum Biology, Institute for Open and Transdisciplinary Research Initiatives, Osaka University, Osaka 560-8531, Japan. ⁴Advanced ICT Research Institute, National Institute of Information and Communications Technology (NICT), Kobe, Hyogo 651-2492, Japan. ⁵Graduate School of Engineering, Kobe University, 1-1 Rokko-dai cho, Nada-ku, Kobe 657-0013, Japan. ⁶Graduate School of Engineering, Nagoya University, Furo-cho, Chikusa-ku, Nagoya 464-8603, Japan. ⁷JST PRESTO, 4-1-8 Honcho, Kawaguchi, Saitama 332-0012, Japan. ⁸Photon Science Center, The University of Tokyo, Bunkyo-ku, Tokyo 113-8656, Japan. ⁹Institute for Photon Science and Technology, School of Science, The University of Tokyo, Bunkyo-ku, Tokyo 113-0033, Japan. [✉]email: miyanishi@qi.mp.es.osaka-u.ac.jp

wave-cw) pumped spontaneous parametric down conversion (SPDC) and the ancillary light pulse prepared by a mode-locked laser. In general, precise spectral-temporal mode matching is necessary for achieving high-visibility quantum interference between independent light sources²⁸, since the coherence time of SPDC photons is in the order of ps to sub ns^{29–31}. In our system, cw-pumped SPDC with time-resolved measurement³² achieves temporal mode matching with reference laser without active synchronisation. The use of the coherent light pulse realises spectral mode matching with the cw-pumped SPDC photon by using conventional frequency filters. This cw-pulse hybrid scheme will be useful for connecting different physical systems at a distance.

RESULTS

Counter-propagation DFS protocol

In this section, we explain the DFS protocol for sharing an entangled photon pair through two single-mode fibres (SMFs)²⁶. We assume that the SMFs are lossy collective noise channels, i.e. the noise varies slowly compared to the propagation time of the photons forming the DFS such that the effect of temporal fluctuation of the noise during that period is negligibly small. No assumptions are needed for the correlation between the fluctuations in the two SMFs. As shown in Fig. 1a, first, the sender Alice prepares a maximally entangled photon pair $|\Phi^+\rangle_{AB} = (|HH\rangle_{AB} + |VV\rangle_{AB})/\sqrt{2}$, while the receiver Bob prepares an ancillary photon $|D\rangle_R$. Here, $|H\rangle$, $|V\rangle$ and $|D\rangle$ represent horizontal (H), vertical (V) and diagonal (D) polarisation states of a photon. Then, Alice sends photon B to Bob through two SMFs after splitting the H- and V-polarised components of the photon B by using a polarisation beam splitter (PBS_A). Bob sends his photon R to Alice in the same way. After the transmission through the SMFs, the separated H- and V-polarised components of the photons B (R) are recombined by the PBS_{B(A)} at Bob's (Alice's) side.

From the assumption of the collective noises, the transformation of the polarisation state formed by photons A, B and R in the

SMFs is expressed as

$$\begin{aligned} |\Phi^+\rangle_{AB} \otimes |D\rangle_R \rightarrow & \frac{1}{2} (\alpha_{H,H}^f |HH\rangle_{AB} + \alpha_{H,V}^f |HV\rangle_{AB} \\ & + \beta_{V,H}^f |VH\rangle_{AB} + \beta_{V,V}^f |VV\rangle_{AB}) \\ & \otimes (\alpha_{H,H}^b |H\rangle_R + \alpha_{H,V}^b |V\rangle_R \\ & + \beta_{V,H}^b |H\rangle_R + \beta_{V,V}^b |V\rangle_R), \end{aligned} \quad (1)$$

where $\alpha_{ij}^{f(b)}$ is the probability amplitude with which the i -polarised photon is transformed into the j -polarised photon through the forward (backward) propagation in the SMF_↑ and $\beta_{ij}^{f(b)}$ is the same for SMF_↓. In the reciprocal media such as SMFs, $\alpha_{H,H}^f = \alpha_{H,H}^b := \alpha_H$ and $\beta_{V,V}^f = \beta_{V,V}^b := \beta_V$ hold²⁶. After passing through the SMF_↑ and SMF_↓, the H and V polarisation photons are respectively extracted from the lower ports of PBS_A and PBS_B, and the photon flipped in the SMFs are discarded. Namely, the terms concerning $\alpha_{H,V}^{f(b)}$, $\alpha_{V,H}^{f(b)}$, $\beta_{H,V}^{f(b)}$ and $\beta_{V,H}^{f(b)}$ are dropped. Then, Alice and Bob obtain an unnormalized state as

$$\begin{aligned} |\Psi\rangle_{AB'R'} = & \frac{1}{2} (\alpha_H^2 |HHH\rangle_{AB'R'} + \beta_V^2 |VVV\rangle_{AB'R'} \\ & + \alpha_H \beta_V |HHV\rangle_{AB'R'} + \alpha_H \beta_V |VVH\rangle_{AB'R'}). \end{aligned} \quad (2)$$

The latter two terms in Eq. (2) are extracted by performing the quantum parity check (QPC)³³ on photons A and R' in Alice's side as shown in Fig. 1b. The Kraus operators K and \bar{K} for the successful and failure events of the QPC are described by $K = |HH\rangle_{A'R'} \langle HV|_{AR'} + |VV\rangle_{A'R'} \langle VH|_{AR'}$ and $\bar{K} = \sqrt{I - K^\dagger K}$, respectively. When Alice performs projective measurement $\{|D\rangle\langle D|, |A\rangle\langle A|\}$ on the photon in mode R'', the remaining polarisation state shared between Alice and Bob becomes $|\Phi^+\rangle_{A'B'}$ or $|\Phi^-\rangle_{A'B'}$ according to the measurement result, where $|\Phi^-\rangle_{A'B'} = (|HH\rangle_{A'B'} - |VV\rangle_{A'B'})/\sqrt{2}$. $|\Phi^-\rangle$ can be converted to $|\Phi^+\rangle$ by performing phase flip operation on photon A'. The overall successful probability of this scheme is $|\alpha_H|^2 |\beta_V|^2 / 2$.

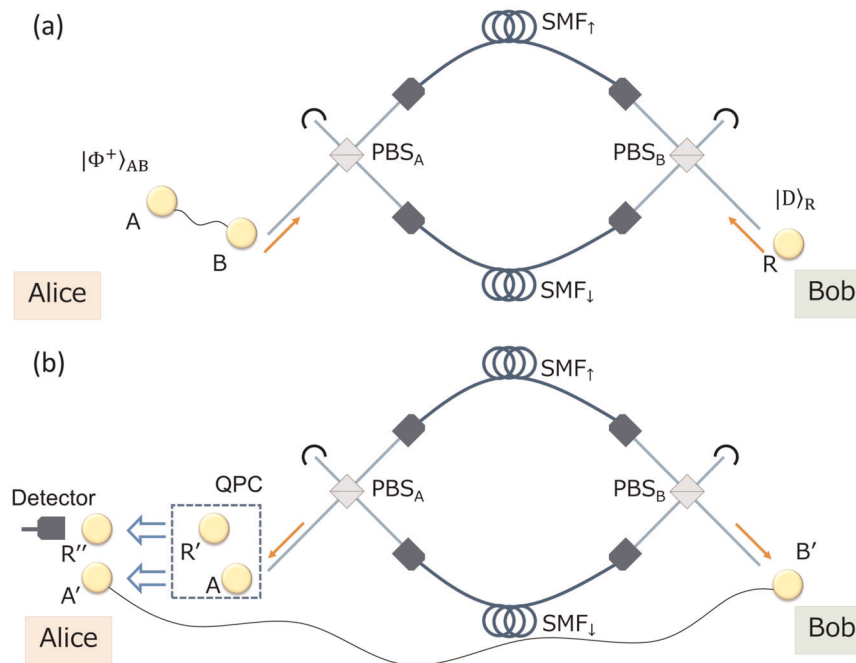


Fig. 1 Schematic diagram of entanglement distribution protocol using counter-propagating ancillary photons. a Alice prepares $|\Phi^+\rangle_{AB}$ and send photon B to Bob. Bob prepares a diagonally polarised ancillary photon R, and sends it to Alice. **b** After the transmission of the SMFs, Alice performs the QPC on photons A and R.

Assuming that the phase shifts and polarisation rotations are completely random and the transmittance of a single photon for each mode is $T = |\alpha_H|^2 = |\beta_V|^2$, the probability with which photon B and R transmit the lossy channels is $\mathcal{O}(T^2)$. This probability is improved to $\mathcal{O}(T)$ by using coherent light pulse with an average photon number of μT^{-1} at Bob's side instead of the single ancillary photon^{25,26}. In the experiment, the entangled photon pairs are prepared by the SPDC with the photon pair generation probability γ . At this average photon number, the condition for suppressing the accidental coincidence events caused by the multi-photon emission is $1 \gg \mu \gg \gamma$ ^{25,27}.

Experimental setup

The experimental setup is shown in Fig. 2. At Alice's side, an entangled photon pair in $|\Phi^+\rangle$ at 1560 nm is generated by the SPDC. For this, a periodically poled lithium niobate waveguide (PPLN/W) (NTT Electronics) is placed in the Sagnac interferometer with a PBS³⁴, and 7-mW cw light at 780 nm with a diagonal polarisation is injected as pump light. The pump light is removed from the SPDC photons by a dichroic mirror (DM1). At a half beam splitter (HBS_A), the SPDC photons are divided into two different spatial paths P1 and P2 with probability 1/2 and the entangled photon pair in $|\Phi^+\rangle$ is prepared. We call the photon in path P2 as photon A and the photon in path P1 as photon B. We note that there are cases where the SPDC photon pair take the same path P1 or P2, but these events are removed by coincidence measurements which are described later.

Photon A is fed to the QPC circuit which we describe later. H- and V-polarised components of the photon B are divided by PBS_A and sent to Bob through 1 km SMF₁ and SMF₁. After passing through the SMFs, they are recombined at PBS_B. The photon in mode B' extracted from the lower port of PBS_B goes to photon detector D_{B'}.

At Bob's side, a weak coherent light pulse at 1560 nm is prepared for an ancillary photon R by difference frequency generation (DFG) at another PPLN/W. The signal light for DFG comes from a Ti:sapphire (Ti:S) laser at 781 nm (pulse width of 100 fs and repetition rate of 80 MHz (Mai Tai, Spectra-Physics)) after a volume holographic grating (VHG1) with a bandwidth of 0.3 nm (ONDAX). The cw pump light at 1563 nm is prepared by DFB laser (NTT Electronics) amplified to a power of 120 mW. After the DFG process, the 1563 nm pump light and the remaining 781 nm light are separated from the converted 1560 nm light by VHG2 with a bandwidth of 1 nm (ONDAX). The DFG light is set to a diagonal polarisation by a HWP and sent to Alice in the same way as photon B through the two SMFs after reflected by a glass plate (GP) with a reflectance of 5%. After the transmission, the light

pulse from the lower port of the PBS_A passes through the HBS_A, and then goes to the QPC circuit.

At the QPC circuit, the H and V component of the coherent light pulse for photon R' are flipped by the HWP, and the light meets another photon A at the PBS. Alice projects the photons in the output mode R'' of the PBS onto the diagonal polarisation by a HWP and a PBS. Finally, when Alice postselects the cases where at least one photon is detected at D_{R''} and D_{A'} and Bob postselects the cases where at least one photon is detected at D_{B'}, a maximally entangled state $|\Phi^+\rangle$ is shared between the modes A' and B'. We used superconducting nanowire single-photon detectors (SNSPDs) for D_{A'}, D_{B'} and D_{R''}. The timing jitter of these SNSPDs is 85 ps each³⁵. To attain a high-fidelity QPC operation, precise spectral-temporal mode matching between the heralded cw-pumped SPDC photons and the coherent light pulse is required. Regarding the temporal mode matching, thanks to the asynchronous nature of cw-pumped SPDC photons, we can extract the event that the coherent light pulse and the heralded single photon exists at the same time by postprocessing. For the postprocessing, the electric signals from D_{R''}, D_{A'}, D_{B'} and the clock signal from the Ti:S laser are connected to a time-to-digital converter which collects all of timestamps with time slot of 1 ps. Regarding the spectral mode matching, the heralded single photon and the coherent light pulse should be filtered by narrow frequency filters. We inserted frequency filters (Alnair labs) whose bandwidths are 0.1 nm for mode B' and 0.03 nm for modes A' and R''. The coherence time of SPDC photons and coherent light pulse are measured to be 169 and 176 ps.

Experimental results

We first characterised the polarisation state of the initial photon pair in paths P1 and P2 by performing the quantum state tomography³⁶ and using the iterative maximum likelihood estimation³⁷. For this purpose, we inserted a pair of a HWP and a QWP in each output mode just after the HBS_A. The reconstructed density operator ρ_{initial} is shown in Fig. 3a. The observed fidelity of ρ_{initial} to the maximally entangled state defined by $F = \langle \Phi^+ | \rho_{\text{initial}} | \Phi^+ \rangle$ was $F = 0.94 \pm 0.01$. The entanglement of formation (EoF)³⁸ is estimated to be $E = 0.90 \pm 0.04$. This result shows Alice prepares highly entangled photon pairs.

Next, we performed the DFS protocol. The average photon number μ of the coherent light pulse after HBS_A was set to $\mu \approx 3.1 \times 10^{-1}$ per 300-ps time window. The photon pair generation probability γ per coincidence between 300-ps window for idler photons and 100-ps window for signal photons was measured to be $\gamma \approx 9.0 \times 10^{-3}$. The reason for employing large detection

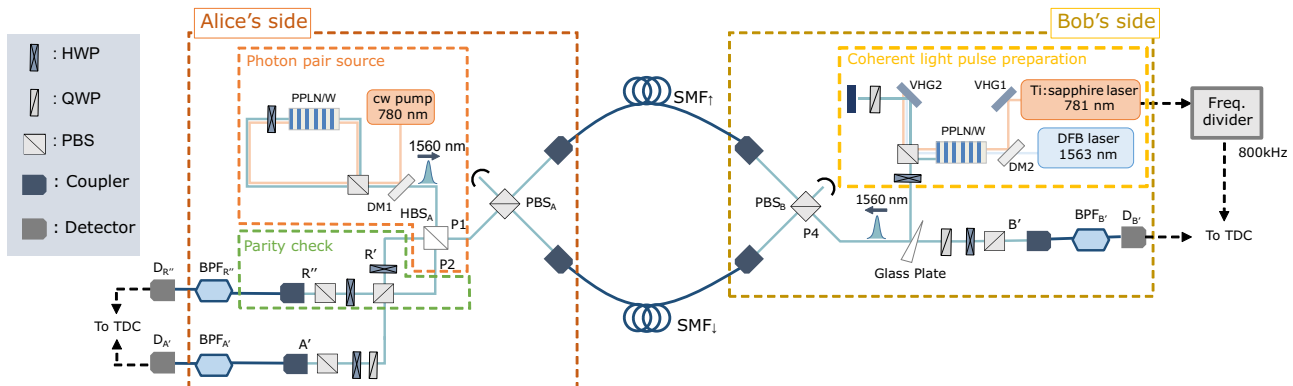


Fig. 2 The experimental setup for our DFS protocol. At Alice's photon pair source, the cw pump light at 780 nm for SPDC is prepared by second-harmonic generation of the light at 1560 nm from an external cavity diode laser with a linewidth of 1.8 kHz. At Bob's ancillary photon source, the pulsed light at 781 nm is filtered by a volume holographic grating (VHG1) with a bandwidth of 0.3 nm and the pulsed light and the cw pump light at 1563 nm are combined by the DM2 and coupled into a PPLN/W. At the data collection stage by TDC, the repetition rate of the electric signal from the Ti:S pulse laser is divided into 800 kHz to reduce the amount of data for avoiding the data overflow.

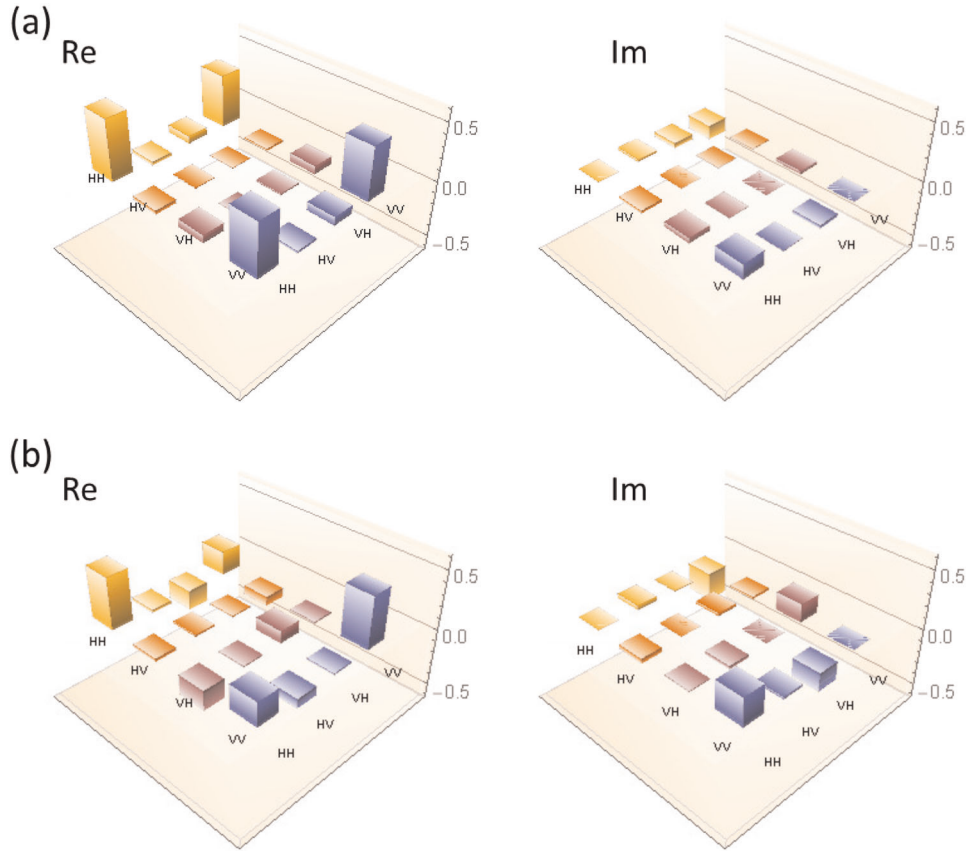


Fig. 3 Reconstructed density matrices. **a** The real part and imaginary part of the ρ_{initial} . **b** The real part and imaginary part of the ρ_{DFS} .

widows for $D_{A'}$ and $D_{R'}$ is to increase the count rate. γ and μ satisfy the condition $1 \gg \mu \gg \gamma$.

Using the threefold coincidence events among $D_{R'}$, $D_{A'}$ and $D_{B'}$ (see Methods), we reconstructed the density operator ρ_{DFS} of the photon pair shared between Alice and Bob. The real part and imaginary part of ρ_{DFS} are shown in Fig. 3b. The observed fidelity to $|\Phi^+\rangle$ was $F = 0.64 \pm 0.1$. The maximised fidelity with the local phase shift defined by $F_\theta = \max_{-\pi \leq \theta \leq \pi} \langle \Phi_\theta^+ | \rho_{\text{DFS}} | \Phi_\theta^+ \rangle$ was $F_\theta = 0.75 \pm 0.10$ with $\theta = -0.87$ rad, where $|\Phi_\theta^+\rangle \equiv (|HH\rangle + e^{i\theta}|VV\rangle)/\sqrt{2}$. This local phase shift between H-polarised photon and V-polarised photon is mainly added by the PBS in the QPC circuit. Accordingly, this phase rotation does not decrease the amount of entanglement since this phase shift does not fluctuate. The EoF for ρ_{DFS} was estimated to be $E = 0.43 \pm 0.19$. The result shows that the DFS scheme protects the entanglement against the collective noise in 1 km of SMF.

DISCUSSION

We discuss the reason for the degradation of the fidelity. Assuming the perfect mode matching between the coherent light pulse and the photon heralded by photon detection at $D_{B'}$, we investigate the influence of multiple photons in the coherent light pulse and the multiple photon pair emission of SPDC on the fidelity. Based on the analysis in ref. ³⁴, we construct a simple theoretical model and derive the relation among the intensity ratio of heralded photon to coherent light pulse, the intensity correlation function $g^{(2)}$ of the heralded photon and the coherent light pulse, and signal to noise ratio of polarisation of the heralded photon. We introduce the polarisation correlation visibilities of the final state defined by $V_Z := |P_{HH} + P_{VV} - P_{HV} - P_{VH}| / (P_{HH} + P_{VV} + P_{HV} + P_{VH})$, $V_X := |P_{DD} + P_{AA} - P_{DA} - P_{AD}| / (P_{DD} + P_{AA} + P_{DA} + P_{AD})$

and $V_Y := |P_{RR} + P_{LL} - P_{RL} - P_{LR}| / (P_{RR} + P_{LL} + P_{RL} + P_{LR})$, where P_{mn} is the coincidence probability among $D_{R'}$ with D-polarisation, D_B with m -polarisation and $D_{A'}$ with n -polarisation. Here, $m, n = H, V, D, A, R, L$, where A, R and L represent antidiagonal polarisation, right circular polarisation and left circular polarisation, respectively. Then, the fidelity of the final state is given by $F = (1 + V_Z + V_X + V_Y)/4$. The explicit formula and detailed derivation are described in the Supplementary Information. We assume that the intensity correlation function $g^{(2)}$ of the stray photons is 2 and that of the coherent light pulse is 1. From the experimental result, the signal to noise ratio of polarisation of the heralded single photon is 56 and the intensity ratio between the heralded single photon and the coherent light pulse is 0.28. By running another experiment, the intensity correlation function of the heralded single photon was estimated to be $g_s^{(2)} = 0.098$. Using these parameters, we estimate the theoretical value of fidelity as 0.81. This value is slightly higher than the experimentally obtained value to be 0.75. We guess the gap of 0.06 is caused by the frequency mode mismatch between the signal photon and the coherent light pulse. If we use optical filters with bandwidths of 0.01 nm^{32,34} or use detectors with timing jitter of less than 60 ps, the influence of the frequency mode mismatch would be < 0.01 . Moreover, by using SPDC photons with smaller $g^{(2)}$ value, and optimisation of the ancillary coherent light pulse intensity would improve the fidelity. For example, when we use SPDC photons with $g_s^{(2)} = 0.05$ (0.01) and the signal to noise ratio of polarisation of the heralded single photon 100 (1000), and optimising the intensity of the coherent light pulse, the theoretical value of fidelity is calculated as 0.86 (0.94), respectively. The detailed simulation of how much fidelity one can expect is presented in Supplementary Material.

In conclusion, we demonstrated the DFS protocol with counter-propagating coherent light pulse generated by a fully

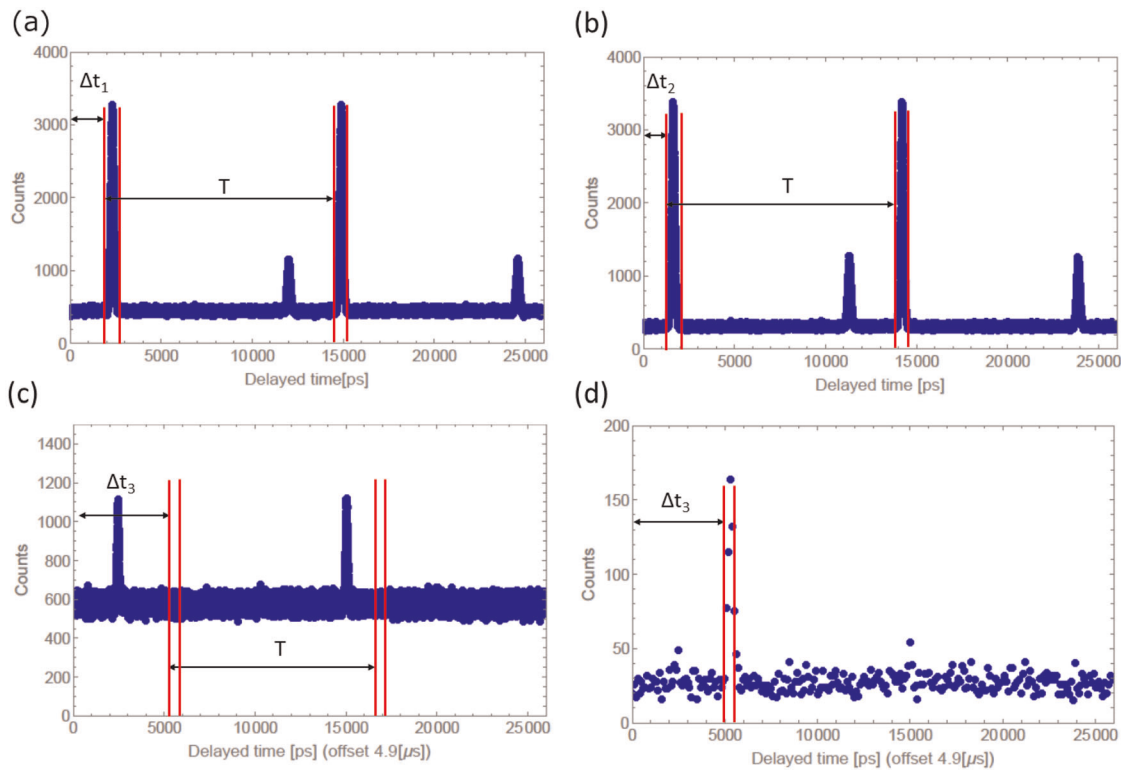


Fig. 4 The delayed counts conditioned by the electric signal from pulse laser. **a–c** correspond to the counts from detector $D_{A'}$, $D_{R'}$ and $D_{B'}$ respectively. The figure **d** shows the delayed counts of $D_{B'}$ conditioned by the photon detection at $D_{A'}$ with delayed time Δt_1 . Each point is integrated for 100 ps in **d**.

independent source at telecom band over 1 km of SMFs. In the demonstration, we employed cw-pulse hybrid system, i.e. a pulsed coherent light source and a continuously emitting photon pair source with time-resolved coincidence measurement, which enables us to perform the DFS scheme without synchronising independent sources. The fidelity of the shared photon pair was 0.75 ± 0.10 , which indicates that entanglement is protected by the DFS after travelling in the SMFs. In practical use, the communication distance of the DFS protocol is limited by the stability of the optical fibre since the noise for the signal photon and the counter-propagating coherent light pulse must satisfy the collective condition. In this regard, a field experiment shows the fluctuations in a 67-km optical fibre are much slower than the round trip time³⁹. We believe that our result will be useful for realising faithful entanglement distribution over a long distance.

METHODS

Data processing

Here, we describe the details of data processing. The threefold coincidence events are obtained as follows. The electric signal from the pulse laser is used as a start signal, and the electric signals from $D_{A'}$, $D_{R'}$ and $D_{B'}$ are used as stop signals. The histograms of the stop signals are shown in Fig. 4a–c. In Fig. 4a, b, a higher peak and a lower peak are observed in every 12.5 ns ($=1/80$ MHz). The higher peak, which is the desired one, is obtained when photon R from Bob transmits the HBS_A. On the other hand, the lower peak as the unwanted peak is obtained when photon R is reflected by the HBS_A and passes through the Sagnac loop. Such unwanted peaks are also observed in Fig. 4c by the photon R coming back to Bob's side after travelling the Sagnac loop. In the experiment, we removed these unwanted detection events by proper settings of the coincidence time windows. Since the entangled photon pairs are emitted continuously, when we postselect the higher peaks in Fig. 4a or b, an additional peak as a counterpart of the photon pair appears at Δt_3 in the delayed signal at $D_{B'}$. As an example, we show the twofold coincidence counts between $D_{A'}$ and $D_{B'}$ in Fig. 4d. We extract the successful events of the DFS protocol by

summing up the threefold coincidence events among $D_{A'}$, $D_{R'}$ and $D_{B'}$ with timings Δt_1 , Δt_2 and Δt_3 , respectively. The widths of the coincidence windows are set to be 300 ps for $D_{A'}$ and $D_{R'}$, and 100 ps for $D_{B'}$, respectively. In this method, the signal photon goes through the fibres after the weak coherent light traverses the fibres in the other direction. Nevertheless, the collective condition still holds, since the optical fibre has negligible fluctuations during the forward and backward propagations.

DATA AVAILABILITY

The experimental data and the source code that support the findings of this study are available from the corresponding author on reasonable request.

Received: 25 October 2019; Accepted: 17 March 2020;

Published online: 20 May 2020

REFERENCES

- Kimble, H. J. The quantum internet. *Nature* **453**, 1023–1030 (2008).
- Wehner, S., Elkouss, D. & Hanson, R. Quantum internet: a vision for the road ahead. *Science* **362**, eaam9288 (2018).
- Gisin, N., Ribordy, G., Tittel, W. & Zbinden, H. Quantum cryptography. *Rev. Mod. Phys.* **74**, 145–195 (2002).
- Lo, H.-K., Curty, M. & Tamaki, K. Secure quantum key distribution. *Nat. Photonics* **8**, 595–604 (2014).
- Sangouard, N., Simon, C., de Riedmatten, H. & Gisin, N. Quantum repeaters based on atomic ensembles and linear optics. *Rev. Mod. Phys.* **83**, 33–80 (2011).
- Cirac, J. I., Ekert, A. K., Huelga, S. F. & Macchiavello, C. Distributed quantum computation over noisy channels. *Phys. Rev. A* **59**, 4249–4254 (1999).
- Broadbent, A., Fitzsimons, J. & Kashefi, E. Universal blind quantum computation. In *2009 50th Annual IEEE Symposium on Foundations of Computer Science*, 517–526 (Atlanta, GA, USA, 2009).
- Brendel, J., Gisin, N., Tittel, W. & Zbinden, H. Pulsed energy-time entangled twin-photon source for quantum communication. *Phys. Rev. Lett.* **82**, 2594–2597 (1999).
- Marcikic, I. et al. Distribution of time-bin entangled qubits over 50 km of optical fiber. *Phys. Rev. Lett.* **93**, 180502 (2004).

10. Inagaki, T., Matsuda, N., Tadanaga, O., Asobe, M. & Takesue, H. Entanglement distribution over 300 km of fiber. *Opt. Express* **21**, 23241–23249 (2013).
11. Sun, Q.-C. et al. Entanglement swapping over 100 km optical fiber with independent entangled photon-pair sources. *Optica* **4**, 1214–1218 (2017).
12. Hübel, H. et al. High-fidelity transmission of polarization encoded qubits from an entangled source over 100 km of fiber. *Opt. Express* **15**, 7853–7862 (2007).
13. Wengerowsky, S. et al. Passively stable distribution of polarisation entanglement over 192 km of deployed optical fibre. *npj Quantum Inf.* **6**, 5 (2020).
14. Lidar, D. A. & Birgitta Whaley, K. *Decoherence-free subspaces and subsystems* 83–120 (Springer Berlin Heidelberg, Berlin, Heidelberg, 2003).
15. Kwiat, P. G., Berglund, A. J., Altepeter, J. B. & White, A. G. Experimental verification of decoherence-free subspaces. *Science* **290**, 498–501 (2000).
16. Walton, Z. D., Abouraddy, A. F., Sergienko, A. V., Saleh, B. E. A. & Teich, M. C. Decoherence-free subspaces in quantum key distribution. *Phys. Rev. Lett.* **91**, 087901 (2003).
17. Boileau, J.-C., Gottesman, D., Laflamme, R., Poulin, D. & Spekkens, R. W. Robust polarization-based quantum key distribution over a collective-noise channel. *Phys. Rev. Lett.* **92**, 017901 (2004).
18. Bourennane, M. et al. Decoherence-free quantum information processing with four-photon entangled states. *Phys. Rev. Lett.* **92**, 107901 (2004).
19. Boileau, J.-C., Laflamme, R., Laforest, M. & Myers, C. R. Robust quantum communication using a polarization-entangled photon pair. *Phys. Rev. Lett.* **93**, 220501 (2004).
20. Yamamoto, T., Shimamura, J., Özdemir, Ş. K., Koashi, M. & Imoto, N. Faithful qubit distribution assisted by one additional qubit against collective noise. *Phys. Rev. Lett.* **95**, 040503 (2005).
21. Chen, T.-Y. et al. Experimental quantum communication without a shared reference frame. *Phys. Rev. Lett.* **96**, 150504 (2006).
22. Prevedel, R. et al. Experimental demonstration of decoherence-free one-way information transfer. *Phys. Rev. Lett.* **99**, 250503 (2007).
23. Yamamoto, T. et al. Experimental ancilla-assisted qubit transmission against correlated noise using quantum parity checking. *N. J. Phys.* **9**, 191 (2007).
24. Yamamoto, T., Hayashi, K., Özdemir, Ş. K., Koashi, M. & Imoto, N. Robust photonic entanglement distribution by state-independent encoding onto decoherence-free subspace. *Nat. Photonics* **2**, 488–491 (2008).
25. Ikuta, R. et al. Efficient decoherence-free entanglement distribution over lossy quantum channels. *Phys. Rev. Lett.* **106**, 110503 (2011).
26. Kumagai, H., Yamamoto, T., Koashi, M. & Imoto, N. Robustness of quantum communication based on a decoherence-free subspace using a counter-propagating weak coherent light pulse. *Phys. Rev. A* **87**, 052325 (2013).
27. Ikuta, R., Nozaki, S., Yamamoto, T., Koashi, M. & Imoto, N. Experimental demonstration of robust entanglement distribution over reciprocal noisy channels assisted by a counter-propagating classical reference light. *Sci. Rep.* **7**, 4819 (2017).
28. Kaltenbaek, R., Blauensteiner, B., Żukowski, M., Aspelmeyer, M. & Zeilinger, A. Experimental interference of independent photons. *Phys. Rev. Lett.* **96**, 240502 (2006).
29. Tanida, M., Okamoto, R. & Takeuchi, S. Highly indistinguishable heralded single-photon sources using parametric down conversion. *Opt. Express* **20**, 15275–15285 (2012).
30. Jin, R.-B. et al. Nonclassical interference between independent intrinsically pure single photons at telecommunication wavelength. *Phys. Rev. A* **87**, 063801 (2013).
31. Tsujimoto, Y. et al. Extracting an entangled photon pair from collectively decohered pairs at a telecommunication wavelength. *Opt. Express* **23**, 13545–13553 (2015).
32. Tsujimoto, Y. et al. High-fidelity entanglement swapping and generation of three-qubit ghz state using asynchronous telecom photon pair sources. *Sci. Rep.* **8**, 1446 (2018).
33. Pittman, T. B., Jacobs, B. C. & Franson, J. D. Probabilistic quantum logic operations using polarizing beam splitters. *Phys. Rev. A* **64**, 062311 (2001).
34. Tsujimoto, Y. et al. High visibility hong-ou-mandel interference via a time-resolved coincidence measurement. *Opt. Express* **25**, 12069–12080 (2017).
35. Miki, S., Yamashita, T., Terai, H. & Wang, Z. High performance fiber-coupled NbTiN superconducting nanowire single photon detectors with Gifford-McMahon cryocooler. *Opt. Express* **21**, 10208–10214 (2013).
36. James, D. F. V., Kwiat, P. G., Munro, W. J. & White, A. G. Measurement of qubits. *Phys. Rev. A* **64**, 052312 (2001).
37. Řeháček, J., Hradil, Z., Knill, E. & Lvovsky, A. I. Diluted maximum-likelihood algorithm for quantum tomography. *Phys. Rev. A* **75**, 042108 (2007).
38. Wootters, W. K. Entanglement of formation of an arbitrary state of two qubits. *Phys. Rev. Lett.* **80**, 2245–2248 (1998).
39. Zhou, C., Wu, G., Chen, X. & Zeng, H. plug and play quantum key distribution system with differential phase shift. *Appl. Phys. Lett.* **83**, 1692–1694 (2003).

ACKNOWLEDGEMENTS

This work was supported by CREST, JST JPMJCR1671; MEXT/JSPS KAKENHI Grant Number JP18H04291, JP18K13483 and JP18K13487. K.M. is supported by JSPS KAKENHI No. 19J10976 and Program for Leading Graduate Schools: Interactive Materials Science Cadet Program.

AUTHOR CONTRIBUTIONS

K.M., Y.T. and R.I. designed the experiment, carried out the experiments under the supervision of T.Y., M.K. and N.I. S.M., M.Y., T.Y. and H.T. developed the system of the superconducting single-photon detectors. All authors analysed the experimental results and contributed to the discussions and interpretations. K.M. wrote the manuscript with input from all authors.

COMPETING INTERESTS

The authors declare no competing interests.

ADDITIONAL INFORMATION

Supplementary information is available for this paper at <https://doi.org/10.1038/s41534-020-0273-5>.

Correspondence and requests for materials should be addressed to K.M.

Reprints and permission information is available at <http://www.nature.com/reprints>

Publisher's note Springer Nature remains neutral with regard to jurisdictional claims in published maps and institutional affiliations.



Open Access This article is licensed under a Creative Commons Attribution 4.0 International License, which permits use, sharing, adaptation, distribution and reproduction in any medium or format, as long as you give appropriate credit to the original author(s) and the source, provide a link to the Creative Commons license, and indicate if changes were made. The images or other third party material in this article are included in the article's Creative Commons license, unless indicated otherwise in a credit line to the material. If material is not included in the article's Creative Commons license and your intended use is not permitted by statutory regulation or exceeds the permitted use, you will need to obtain permission directly from the copyright holder. To view a copy of this license, visit <http://creativecommons.org/licenses/by/4.0/>.

© The Author(s) 2020